Materials Research Bulletin 45 (2010) 15–20

Contents lists available at ScienceDirect

Materials Research Bulletin

journal homepage: www.elsevier.com/locate/matresbu

Synthesis, characterization and properties of carbon nanotubes microspheres from pyrolysis of polypropylene and maleated polypropylene

Junhao Zhang [a,b,*], Jin Du [b], Yitai Qian [b], Shenglin Xiong [b]

[a] School of Materials Science and Engineering, Jiangsu University of Science and Technology, Zhenjiang Jiangsu 212003, People's Republic of China
[b] Department of Chemistry, University of Science and Technology of China, Heifei, Anhui 230026, People's Republic of China

ARTICLE INFO

Article history:
Received 18 April 2009
Received in revised form 2 September 2009
Accepted 11 September 2009
Available online 22 September 2009

Keywords:
A. Nanostructures
C. Electron microscopy
C. Raman spectroscopy
D. Catalytic properties

ABSTRACT

Microspheres assembled from carbon nanotubes (MCNTs), with the diameters ranging from 5.5 to 7.5 μm, were synthesized by means of pyrolysis of polypropylene and maleated polypropylene in an autoclave. The characterization of structure and morphology was carried out by X-ray diffractometer (XRD), field-emission scanning electron microscopy (FESEM), (high resolution) transmission electron microscope [(HR)TEM)], selected-area electron diffraction (SAED) and Raman spectrum. As a typical morphology, the possible growth process of MCNTs was also investigated and discussed. The results of nitrogen adsorption–desorption indicate that the Brunauer–Emett–Teller (BET) surface area (140.6 m^2/g) of the MCNTs obtained at 600 °C is about twice as that (74.5 m^2/g) of carbon nanotubes obtained at 700 °C. The results of catalytic experiment show that MCNTs based catalyst has higher catalytic activity than the carbon nanotubes based catalyst for the preparation of methanol and dimethoxy-ethane by oxidation of dimethyl ether.

1. Introduction

In recent years, there has been increasing interest in preparation and processing of various nanostructured carbon materials. Difficulties for functionalizing carbon nanotubes (CNTs) and limitations in processing methods are main barriers for the pursuit of these potential applications. For these reasons, new development to assemble and align CNTs is still a great and fascinating challenge. To date, synthesis of CNTs is reported via various methods, such as laser vaporization, arc discharge, pyrolysis, chemical vapor deposition (CVD) and solvothermal processes [1–7].

The properties of carbon materials are strongly influenced by their morphologies and structures. Hence, the fabrication of carbon materials with a particular morphology and well-defined structure is very important for their various properties-related applications. Hou et al. prepared helically coiled CNTs using $Fe(CO)_5$ as floating catalyst precursor [8]. Bajpai and co-workers synthesized large-scale aligned/micropatterned straight CNTs by pyrolysis of iron(II) phthalocyanine on the pristine quartz glass plates in a tube furnace [9]. Moreover, hollow carbon microspheres were also prepared by a variety of methods [10–12], and aligned mule-walled carbon nanotubes and porous hollow CNTs composite cages were also produced by a layer-by-layer assembly and templating technique [13,14]. In addition, sea urchin-like nanostructured carbon spheres were fabricated from the growth of CNTs bundles on hollow carbon spheres by CVD with monodispersed iron oxide nanoparticles as the catalyst [15].

Polymeric materials are frequently used as carbon sources for the preparation of CNTs [16–19]. For example, Tang and co-workers synthesized multiwalled carbon nanotubes in large quantities by burning a polypropylene/nickel/montmorillonite composite in the atmosphere [20–23]. He and co-workers synthesized carbon nanotubes, chestnut-like carbon nanotube spheres and carbon nanospheres from catalytic pyrolysis of polypropylene (PP) using different catalyst precursors [24,25]. In their methods, it is necessary that catalyst precursors were mixed with PP and clay, then such nanocomposites were burned to obtain carbon nanotubes. Otherwise no CNTs were formed. In this article, we report a simple pyrolysis method to synthesize MCNTs, using PP as carbon source and maleated polypropylene (MA-PP) as compatibilizer and carbon source, and ferrocene as catalyst precursor without pre-mixing all components. The growth mechanism of MCNTs was investigated by FESEM and proposed here. The catalytic activities of the MCNTs based catalysts and CNTs based catalysts have been tested by preparation of methanol and dimethoxy-ethane (DMET) from dimethyl ether (DME), showing that the MCNTs based catalysts exhibit higher catalytic activity than CNTs based catalysts.

* Corresponding author at: School of Materials Science and Engineering, Jiangsu University of Science and Technology, Zhenjiang Jiangsu 212003, People's Republic of China. Fax: +86 511 3631760.
E-mail address: jhzhang6@mail.ustc.edu.cn (J. Zhang).

0025-5408/$ – see front matter © 2009 Elsevier Ltd. All rights reserved.
doi:10.1016/j.materresbull.2009.09.007

2. Experimental

All chemicals used in this work, such as ferrocene [$Fe(C_5H_5)_2$] are A. R. regents from the Shanghai Chemical Factory (China). PP (F401) is supplied as pellets by Yangzi Petrochemical Co. (China). MA-PP is supplied by Chemical Material Co., Ltd. (China), and the grafting yield of maleic anhydride groups is 4 phr and its M_w measured by Gel Permeation Chromatograph (GPC) is 30,000.

In a typical experiment, ferrocene (0.50 g), PP (2.00 g, pellets with diameters of about 4 mm) and MA-PP (0.50 g, pellets with diameters of about 4 mm) were added into an autoclave reactor of 20 mL without pre-mixing the components. The reactors were sealed and maintained at 600 and 700 °C for 12 h, and then allowed to cool to room temperature naturally. The dark products were collected and washed with dilute HCl aqueous solution, ethanol, and distilled water. The final products were dried in a vacuum at 60 °C for 6 h.

TiO_2/CNTs, TiO_2/MCNTs, CuO/CNTs and CuO/MCNTs catalysts were prepared by wet impregnation with an aqueous solution of cupric nitrate and an ethanol solution of analytical tetrabutyl titanate to give CuO and TiO_2 content of 10%, respectively. After 12 h, the obtained solid samples were firstly dried at 100 °C in air for 12 h and then calcined at 500 °C in air for 3 h. The obtained samples were used to test their catalytic properties.

The XRD patterns of the products were recorded on a Rigaku (Japan) D/max-γA X-ray diffractometer equipped with graphite monochromatized Cu Kα radiation (λ = 1.54178 Å). The Raman spectrums were investigated at ambient temperature on a Spex 1403 Raman spectrometer (Ar ion laser, 514.5 nm). The FESEM images of the products were examined by a field-emission scanning electron microscope (JEOL-6300F). The TEM and HRTEM images and the SAED patterns were taken on a JEOL 2010 high resolution transmission electron microscope at an acceleration voltage of 200 kV. The nitrogen adsorption–desorption isotherms and textural properties were determined by Beckman Coulter SA3100.

Catalytic experiments were carried out in a continuous flow fixed-bed quartz reactor (8 mm i.d.) under atmospheric pressure. 0.3 g catalysts of 40–60 mesh size were loaded, and the catalysts were pretreated using the mixed gas of 17% O_2 and 83% He for 1 h at 350 °C. A feed gas mixture of 42% DME, 8% O_2 and 50% He was introduced with a space velocity of 3480 mL g^{-1} h^{-1}. The effluent was held at 383 K and analyzed on-line by gas chromatographs.

3. Results and discussion

As shown in Fig. 1a, XRD patterns of the products prepared at 600 and 700 °C for 12 h both have two peaks, which can be indexed as (0 0 2) and (1 0 0) reflections of hexagonal graphite (JCPDS Card Files, No. 41-1487). Compared with the (0 0 2) peaks, it indicates the better crystallinity of the product obtained at 700 °C than that of the product obtained at 600 °C. Fig. 1b gives their corresponding Raman spectra, showing two similar Raman bands at 1346 cm^{-1} (D band) and 1600 cm^{-1} (G band). More specifically, the two peaks exhibit an E_{2g} mode of graphite related to the vibration of sp^2-bonded carbon atoms in a 2D hexagonal lattice (such as in a grapheme layer) and A_{1g} mode of graphite related to the disorder features due to the finite particle size effect or lattice distortion of the graphite crystals, respectively [26–28]. Based on the previous research results [29] and the present Raman spectra, it can be rationally speculated that the graphitic layers contained in the product prepared at 700 °C are more regular than that contained in the product prepared at 600 °C.

Typical FESEM images in Fig. 2 indicate that large amounts of MCNTs and CNTs were produced by pyrolysis of PP and MA-PP at 600 and 700 °C. Fig. 2a displays the MCNTs with diameters ranging from 5.5 to 7.5 μm, and single microsphere with the diameter of 6.3 μm is shown in Fig. 2b. The magnified FESEM image in Fig. 2c give more information of the MCNTs' surface, which reveals that these microsphere are composed of CNTs with diameters in the range of 35–55 nm. Fig. 2d, which is the magnified image of region 1 in Fig. 2c, shows that the obtained products include about 4% carbon nanoparticles according to the FESEM observation. Fig. 2e, which is the magnified image of region 2 in Fig. 2c, shows that the surface of MCNTs is rough. However, at the higher temperature of 700 °C, large amounts of CNTs with length of several micrometers to tens of micrometers are obtained instead of microspheres, as presented in Fig. 2f and g. Through careful observation of these images, the carbon nanotubes have smooth and clean surface with the diameters ranging from 40 to 70 nm.

Fig. 3a is the TEM image of a MCNT with the diameter of about 6 μm prepared at 600 °C. Fig. 3d shows that the inner diameters of the carbon nanotubes prepared at 700 °C are between 7 and 30 nm, and the outer diameters are between 40 and 70 nm, as well as few thinner nanotubes were also observed. Fig. 3b and e displays two individual nanotubes. From the comparison of the two individual CNTs displayed in Fig. 3b and e, it is found that the wall of the CNT obtained at 600 °C is rougher than that of the CNT obtained at 700 °C. To further characterize the wall structure of the as-synthesized CNTs, more detailed studies are executed by HRTEM. Fig. 3c and f shows HRTEM images for the wall structures of nanotubes. The interlayer spacings in the walls are about 0.34 nm, corresponds to the (0 0 2) distance of graphitic carbon lattice. From the comparison of Fig. 3c and f, it can be observed that the former has some stacking faults. The SAED patterns (inset in Fig. 3c and f) are characteristic of CNTs, and the two elongated arcs and circle correspond to (0 0 2), (1 0 0) planes of graphite carbon, which are consistent with the XRD and HRTEM results.

A series of relevant experiments have been carried out through altering experimental parameters to investigate the effect of reaction conditions on the formation of MCNTs. It is obvious that

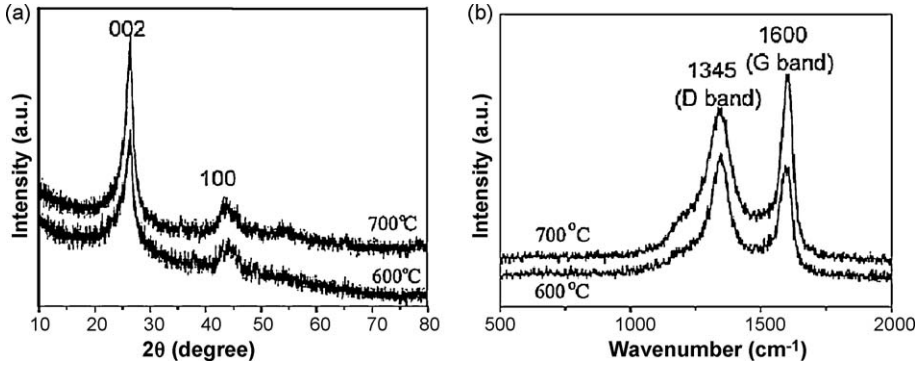

Fig. 1. (a) XRD patterns of the products obtained at 600 °C and 700 °C for 12 h; (b) Raman spectrums of the products obtained at 600 °C and 700 °C for 12 h.

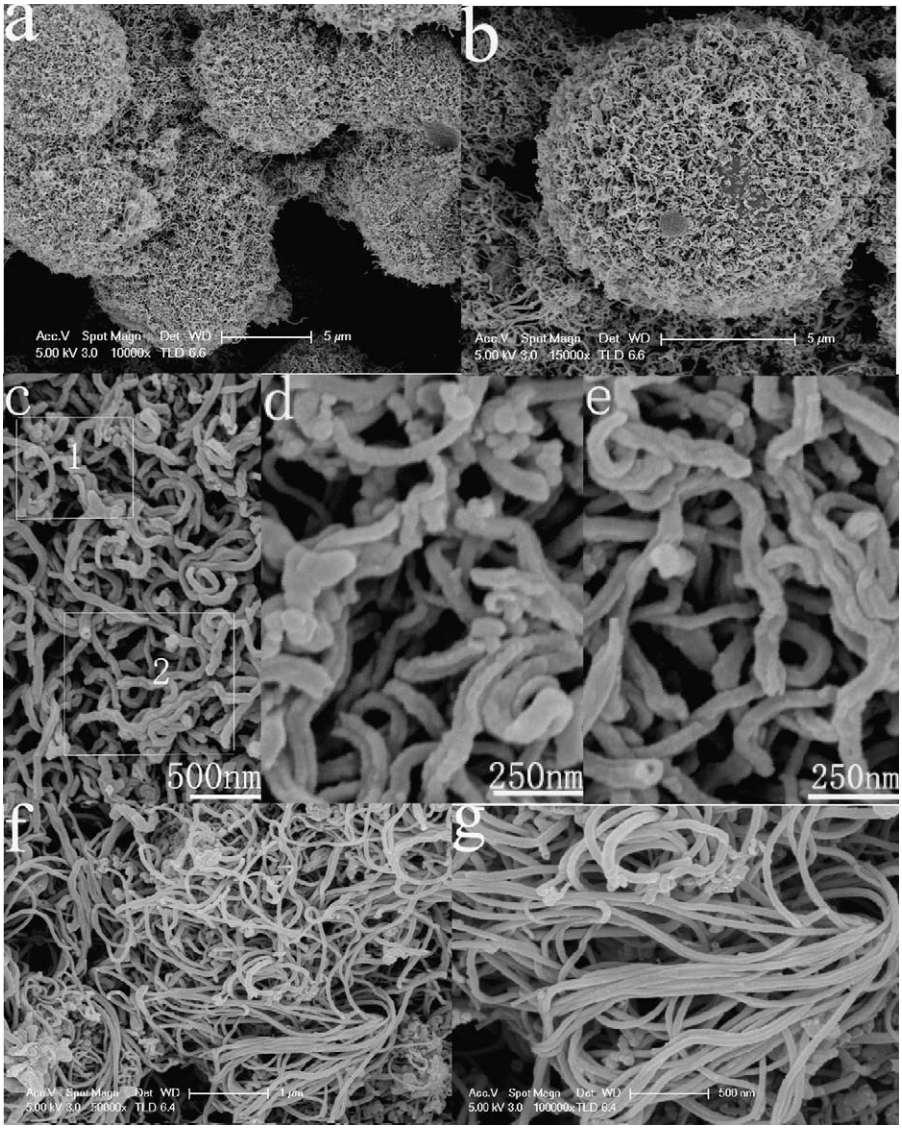

Fig. 2. (a and b) Low magnification FESEM images of MCNTs obtained at 600 °C for 12 h; (c) high magnification FESEM images of the surface of MCNTs obtained at 600 °C for 12 h; (d and e) high magnification FESEM images of regions 1 and 2 in (c); (f and g) Different magnification FESEM images of CNTs obtained at 700 °C for 12 h.

the reaction temperature and time play critical roles in the formation of MCNTs. Lower temperature than 400 °C cannot initiate the reactions. When the reaction temperatures are at 400 and 500 °C for 12 h, the main products are the amorphous carbon materials. At 600 °C for 12 h, a large scale of MCNTs can be observed in product, as shown in Fig. 2a. Raising reaction temperature to 700 °C, abundant CNTs were produced but not assembled into microspheres (see Fig. 2f). To gain a better understanding of the growth process of the MCNTs, the time-dependent samples were collected and studied by FESEM and shown in Fig. 4. After 1, 2 h shown in Fig. 4a and b, the main products are the solid microspheres. As the reaction time was increased to 4 h, many white raised dots on the surface of microspheres are clearly observed, and some dots have openings. With the extension of reaction time, dots on the surface of microspheres become more and more. When reaction time reached 8 h, many CNTs grow out from the spheres. CNTs have become the major component of the microspheres, when reaction time was 10 h.

The mechanisms of formation of MCNTs could be deduced from the above experimental results (Fig. 4), which is similar to the report of Ref. [24]. Ma et al. reported that pure PP and PP nanocomposites formed spheres easily under heating conditions [30]. In our experiment process, PP-MA was used as compatibilizer to improve the dispersion of $Fe(C_5H_5)_2$ in the PP matrix [20,31], and PP and MA-PP may form microspheres containing $Fe(C_5H_5)_2$ after the melting temperature of PP. When the PP/MA-PP/$Fe(C_5H_5)_2$ composite was heated to 400 °C, $Fe(C_5H_5)_2$ (decomposition temperature: 400 °C [32]) decomposes instantly, giving a large number of Fe nanoparticles within the microspheres, which acted as effective and necessary dehydrogenation catalyst in the experiment. The processes of the degradation of polymers and the catalytic decomposition of the pyrolytic species around the Fe particles were endothermic, so the thermal degradation rate of the sphere surface is faster than that of the interior. In addition, the pyrolytic species of the surface were thermally degradated to form carbon layers without catalysts. PP and MA-PP of the interior pyrolyzes to give pyrolytic species that were sealed in an autoclave-like microreactor formed by carbon layers. Within the microreactor, the pyrolytic species were catalyzed to form CNTs on these Fe nanoparticles. The confinement of the microreactor resulted in curled and rough CNTs and eventually formed carbon nanotubes microspheres. However, when the temperature was higher, for example 700 °C, the pyrolysis rate of polymers might be

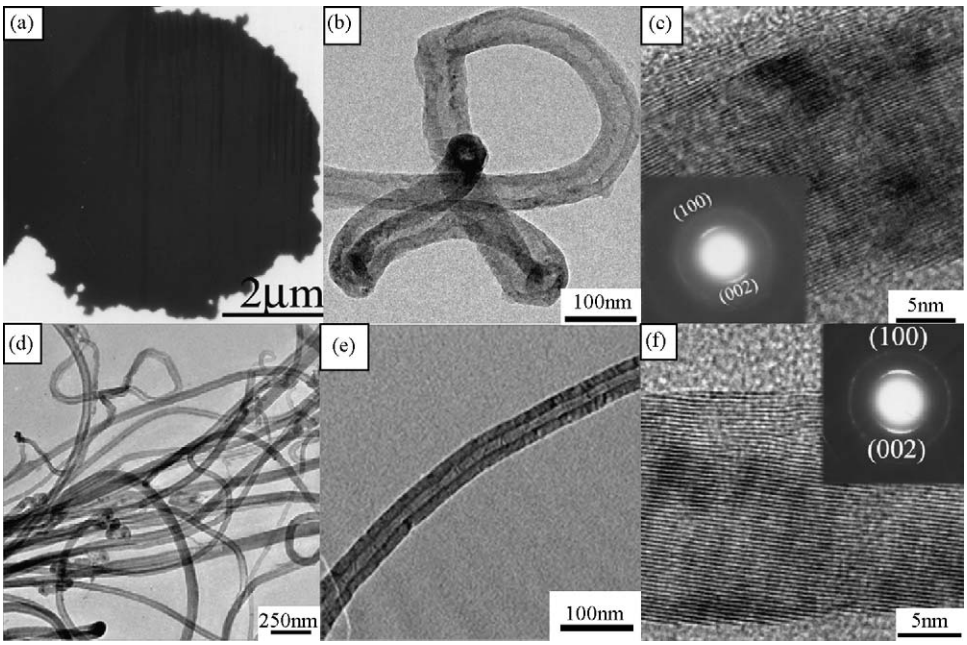

Fig. 3. (a) TEM image of MCNTs obtained at 600 °C for 12 h; (b) TEM image of a single CNT obtained at 600 °C for 12 h; (c) HRTEM image of the CNT and its SAED pattern (inset) obtained at 600 °C for 12 h; (d) TEM images of several CNTs obtained at 700 °C for 12 h; (e) TEM images of a single CNT obtained at 700 °C for 12 h; (f) HRTEM image of the CNT and its SAED pattern (inset) obtained at 700 °C for 12 h.

too fast to result in that the polymer had decomposed completely before carbon layers formed. So the final product is straight and dispersed CNTs without the confinement of the carbon layers, shown in Figs. 2f and 3d.

Fig. 5 shows the nitrogen adsorption–desorption isotherms of the MCNTs and CNTs. The BET surface areas are 140.6 and 74.5 m^2/g, respectively. The calculations of Barrett–Joyner–Halenda (BJH) reveal that the pore-size distribution of MCNTs centers at 44.5 and 4.1 nm, which is more uniform than that of CNTs. It is noteworthy mentioning that the BET surface area of the MCNTs is about twice as that of CNTs. According to the morphology and structure characteristic, the higher BET surface area of MCNTs can be attributed to the smaller diameters, the rough surface of CNTs in MCNTs, the more defects, and the existence of carbon nanoparticles. It is expected that MCNTs based catalyst has higher activity.

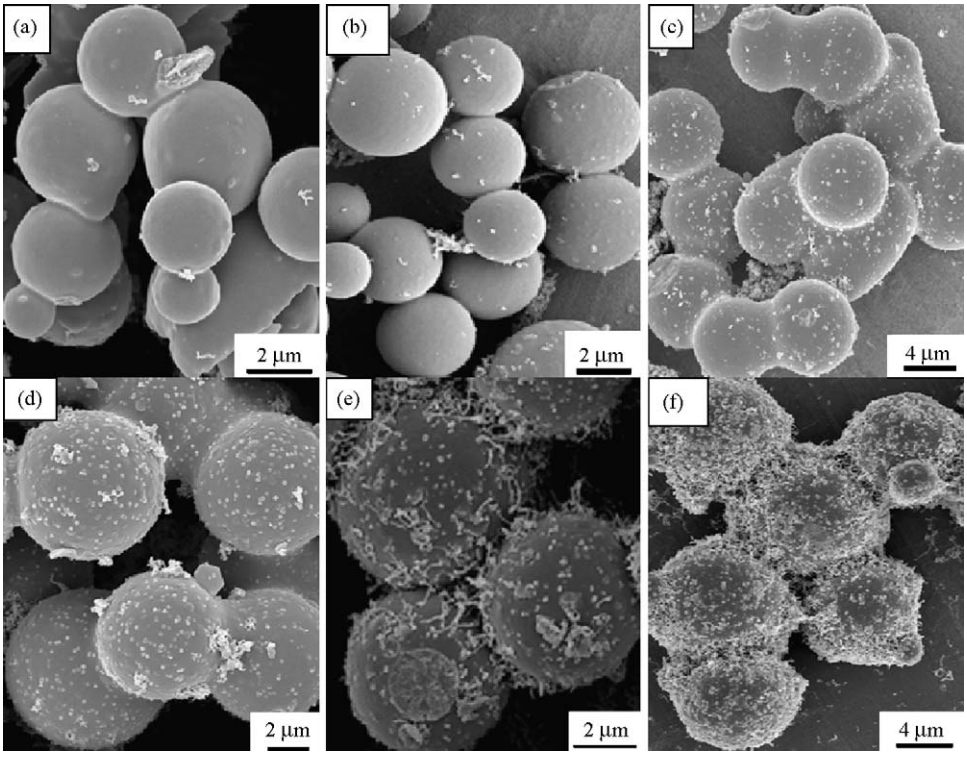

Fig. 4. (a–f) FESEM images of the products obtained at 600 °C for 1, 2, 4, 6, 8 and 10 h, respectively.

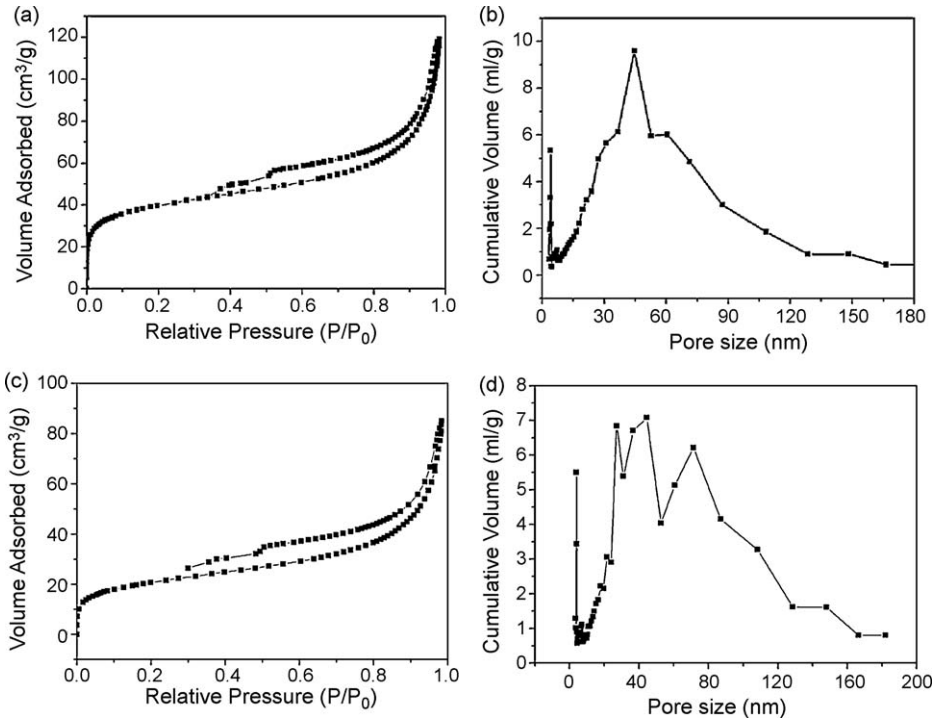

Fig. 5. (a) Typical N_2 adsorption–desorption isotherm of MCNTs obtained at 600 °C; (b) pore size distribution of MCNTs obtained at 600 °C; (c) typical N_2 adsorption–desorption isotherm of CNTs obtained at 700 °C; (d) pore size distribution of CNTs obtained at 700 °C.

In order to investigate the catalytic activity of MCNTs based catalyst, further experiments were carried out to compare the catalytic activities of MCNTs and CNTs based catalysts. MCNTs, CuO(10%)/CNTs, CuO(10%)/MCNTs, TiO_2(10%)/CNTs and TiO_2(10%)/MCNTs catalysts were prepared to test the ability of preparing methanol and DMET from DME. Fig. 6a shows the curves of catalytic performance for the preparation of methanol from DME under the conditions that without catalyst, MCNTs, TiO_2(10%)/CNTs and TiO_2(10%)/MCNTs catalysts, respectively. The results show that the DME conversion and methanol selectivity are very low in the presence of no catalyst or MCNTs as catalyst. The DME conversion and methanol selectivity of TiO_2(10%)/MCNTs are higher than those of TiO_2(10%)/CNTs. The maximum selectivity of methanol is improved 13% and the DME conversion is enhanced about 7% at 300 °C. The catalytic performance of CuO(10%)/CNTs and CuO(10%)/MCNTs catalysts for the partial oxidation of dimethyl ether (DME) to DMET, is also investigated in Fig. 6b. The results demonstrate that DME conversion and DMET selectivity of CuO(10%)/MCNTs are higher than those of CuO(10%)/CNTs. The maximum DMET selectivity is improved from 8.5% to 11.9%, and the DME conversion is enhanced about 4% at 300 °C. However, under the condition of no catalyst or MCNTs as catalyst, the DME conversion is lower than that of CuO(10%)/CNTs or CuO(10%)/MCNTs catalysts; and the DMET selectivity is zero. The above results indicate that effective catalysts are necessary, and higher surface area is a very important factor to improve catalytic activity, which cause the higher adsorption of DME and prolong the residence time of DME on the surface of the catalysts. By comparing the catalytic activity of MCNTs and CNTs based catalysts, the improvement of the catalytic activity of MCNTs based catalyst can be attributed mainly to higher BET surface areas.

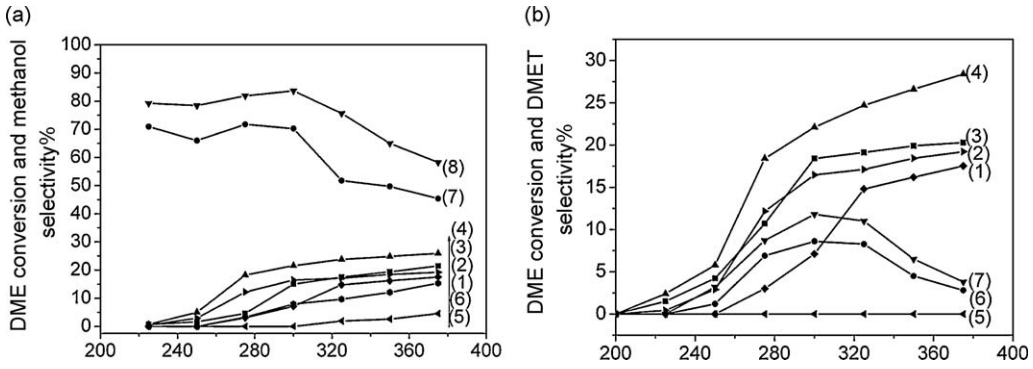

Fig. 6. (a) Catalytic performance of different catalysts: (1) DME conversion without catalyst, (2) DME conversion of MCNTs catalyst, (3) DME conversion of TiO_2/CNTs catalyst, (4) DME conversion of TiO_2/MCNTs catalyst, (5) methanol selectivity without catalyst, (6) methanol selectivity of MCNTs catalyst, (7) methanol selectivity of TiO_2/CNTs catalyst and (8) methanol selectivity of TiO_2/MCNTs catalyst; (b) catalytic performance of different catalysts: (1) DME conversion without catalyst, (2) DME conversion of MCNTs catalyst, (3) DME conversion of CuO/CNTs catalyst, (4) DME conversion of CuO/MCNTs catalyst, (5) DMET selectivity without catalyst and of MCNTs catalyst, (6) DMET selectivity of CuO/CNTs catalyst and (7) DMET selectivity of CuO/MCNTs catalyst.

4. Conclusions

Novel shaped MCNTs have been synthesized by the pyrolysis of PP and MA-PP using $Fe(C_5H_5)_2$ as catalyst precursor at 600 °C in an autoclave. The diameters of MCNTs are about 5.5–7.5 μm. CNTs with highly crystalline nature have also been obtained at 700 °C. The growth mechanism of MCNTs was investigated and discussed on the basis of the experimental results. The results of nitrogen adsorption–desorption indicate that the BET surface area of the MCNTs prepared at 600 °C is about twice as that of CNTs prepared at 700 °C, which results in higher catalytic activity of MCNTs based catalyst for the preparation of methanol and DMET from DME. The results suggest that the catalytic property of carbon materials be related to its structural feature.

Acknowledgements

The authors greatly acknowledge the financial support from the 973 Project of China (Grant No. 2005CB623601) and start fund for advanced professional of Jiangsu University of Science and Technology (No. 35060810).

References

[1] S.H. Liu, R.F. Lu, S.J. Huang, A.Y. Lo, C. Shu-Hua, S.B. Liu, Chem. Commun. 32 (2006) 3435.
[2] Z.L. Li, J. Zhang, Y. Li, Y.J. Guan, Z.C. Feng, C. Li, J. Mater. Chem. 16 (2006) 1350.
[3] J.L. Blacknum, Y. Yan, C. Engtrakul, P.A. Parilla, K. Jones, T. Gennett, A.C. Dillon, M.J. Heben, Chem. Mater. 18 (2006) 2558.
[4] H.X. Qiu, Z.J. Shi, L.H. Guan, L.P. You, M. Gao, S.L. Zhang, J.S. Qiu, Z.N. Gu, Carbon 44 (2006) 516.
[5] F.L. Deepak, A. Govindaraj, C.N.R. Rao, Chem. Phys. Lett. 345 (2001) 5.
[6] M.D. Lima, R. Bonadiman, M.J. de Andrade, J. Toniolo, C.P. Bergmann, Diam. Relat. Mater. 15 (2006) 1708.
[7] J.W. Liu, M.W. Shao, X.Y. Chen, W.C. Yu, X.M. Liu, Y.T. Qian, J. Am. Chem. Soc. 125 (2003) 8088.
[8] H.Q. Hou, Z. Jun, F. Weller, A. Greiner, Chem. Mater. 15 (2003) 3170.
[9] V. Bajpai, L.M. Dai, T. Ohashi, J. Am. Chem. Soc. 126 (2004) 5070.
[10] J.M. Shen, J.Y. Li, Z. Huang, Q. Chen, S.Y. Zhang, Y.T. Qian, Carbon 44 (2006) 2171.
[11] F.B. Zhang, H.L. Li, Mater. Chem. Phys. 98 (2006) 456.
[12] L.C. Li, H.H. Song, X.H. Chen, Carbon 44 (2006) 596.
[13] J.W. Liu, X.J. Li, A. Schrand, T. Ohashi, L.M. Dai, Chem. Mater. 17 (2005) 6599.
[14] L.J. Ji, J. Ma, C.G. Zhao, W. Wei, L.J. Ji, X.C. Wang, M.S. Yang, Y.F. Lu, Z.Z. Yang, Chem. Commun. 11 (2006) 1206.
[15] Y.Z. Piao, K.J. An, J.Y. Kim, T.Y. Yu, T.H. Hyeon, J. Mater. Chem. 16 (2006) 2984.
[16] D. Sarangi, C. Godon, A. Granier, R. Moalic, A. Goullet, O. Chauvet, Appl. Phys. A 73 (2001) 765.
[17] Y.H. Chung, S. Jou, Mater. Chem. Phys. 92 (2005) 256.
[18] H. Nishino, R. Nishida, T. Matsui, N. Kawase, I. Mochida, Carbon 41 (2003) 2819.
[19] U. Arena, M.L. Mastellone, G. Camino, E. Boccaleri, Polym. Degrad. Stab. 91 (2006) 763.
[20] T. Tang, X.C. Chen, X.Y. Meng, H. Chen, Y.P. Ding, Angew. Chem. Int. Ed. 44 (2005) 1517.
[21] R.J. Song, Z.W. Jiang, W.G. Bi, W.X. Cheng, J. Lu, B.T. Huang, T. Tang, Chem. Eur. J. 13 (2007) 3234.
[22] Z.W. Jiang, R.J. Song, W.G. Bi, J. Lu, T. Tang, Carbon 45 (2007) 449.
[23] T. Tang, X.C. Chen, H. Chen, X.Y. Meng, Z.W. Jiang, W.G. Bi, Chem. Mater. 17 (2005) 2799.
[24] X.C. Chen, J.H. He, C.X. Yan, H.M. Tang, J. Phys. Chem. B 110 (2006) 21684.
[25] X.C. Chen, H. Wang, J.H. He, Nanotechnology 19 (2008) 325607.
[26] W.S. Bacsa, D. Ugarte, A. Chatelain, W.A. de Heer, Phys. Rev. B 50 (1994) 15473.
[27] P.C. Eklund, J.M. Holden, R.A. Jishi, Carbon 33 (1995) 959.
[28] Y. Wang, D.C. Alsmeyer, R.L. McCreedy, Chem. Mater. 2 (1990) 557.
[29] A.C. Dillon, A.H. Mahan, P.A. Parilla, J.L. Alleman, M.J. Henen, K.M. Jones, K.E.H. Gilbert, Nano Lett. 3 (2003) 1425.
[30] J.S. Ma, S.M. Zhang, Z.N. Qi, G. Li, Y.L. Hu, J. Appl. Polym. Sci. 83 (2002) 1978.
[31] J.H. Zhang, J. Li, J. Cao, Y.T. Qian, Mater. Lett. 62 (2008) 1839.
[32] M. Bernhauer, M. Braun, K.J. Hüttinger, Carbon 32 (1994) 1073.